JOURNAL OF GEOPHYSICAL RESEARCH, VOL. 112, B08402, doi:10.1029/2005JB004192, 2007

Convection under a lid of finite conductivity: Heat flux scaling and application to continents

C. Grigné,[1] S. Labrosse,[2] and P. J. Tackley[1]

Received 28 November 2005; revised 12 April 2007; accepted 30 April 2007; published 1 August 2007.

[1] A scaling law for the heat flux out of a convective fluid covered totally or partially by a finitely conducting lid is proposed. This scaling is constructed in order to quantify the heat transfer out of the Earth's mantle, taking into account the effect of the dichotomy between oceans and continents, which imposes heterogeneous thermal boundary conditions at the surface of the mantle. The effect of these heterogeneous boundary conditions is studied here using simple two-dimensional models, with the mantle represented by an isoviscous fluid heated from below and continents represented by nondeformable lids of finite thermal conductivity set above the surface of the model. We use free-slip boundary conditions under the oceanic and continental zones in order to study in an isolated way the possible thermal effect of continents, independently of all mechanical effect. A systematic study of the heat transfer as a function of the Rayleigh number of the fluid, of the width of the lid, and of its thermal properties is carried out. We show that estimates of continental lithosphere thickness imply a strong insulating effect from continents on mantle heat loss, at least locally. The heat flux below continents was low in the past and of the order of the present one if the continental thickness has remained broadly constant over the Earth's history.

Citation: Grigné, C., S. Labrosse, and P. J. Tackley (2007), Convection under a lid of finite conductivity: Heat flux scaling and application to continents, *J. Geophys. Res.*, *112*, B08402, doi:10.1029/2005JB004192.

1. Introduction

[2] The clear dichotomy at the surface of the Earth between oceans and continents implies heterogeneous boundary conditions at the surface of the convective mantle. The oceanic lithosphere is recycled into the mantle, and can be considered as the active upper thermal boundary layer of the mantle. Continents, due to their chemical buoyancy and to their strength, do not participate in mantle convection. Estimates of mantle heat flux under stable continental shields are low, of the order of 7–15 mW m^{-2} [*Pinet et al.*, 1991; *Guillou et al.*, 1994; *Jaupart et al.*, 1998], while the mean oceanic heat flux is close to 100 mW m^{-2}, which indicates a strong insulating effect of continents on mantle heat loss.

[3] We construct a scaling law for the heat flux out of a system covered either partially or totally by a lid of finite conductivity, which represents a continent. The purpose of the present study is to better understand the ratio between the continental and the oceanic heat flux in the present Earth and in the past. While the mantle was hotter in the past, yielding higher heat flux, geochemical data suggest that continental geothermal gradients in the Archean were not much different from present ones [*Bickle*, 1978; *England and Bickle*, 1984; *Boyd et al.*, 1985]. We aim to study this counterintuitive feature, referred to as "the Archean paradox," with an approach that takes into account the different thermal boundary conditions seen by the mantle below oceans and below continents.

[4] A better understanding of the heat transfer in a system with two types of thermal boundary condition is also important in reconstructions of the thermal history of the Earth. Several studies [e.g., *Christensen*, 1985; *Conrad and Hager*, 1999; *Korenaga*, 2003; *Grigné et al.*, 2005] have pointed out the contradictions between geochemical data and geophysical parameterized approaches that track back the history of heat loss out the Earth's mantle: Standard parameterized models predict a too rapid cooling of the Earth at the beginning of its history, leading to a low present-day secular cooling rate, which, added to the internal heat production derived from geochemical estimates of radioactive elements concentrations in the mantle, cannot explain the observed present-day heat loss of the Earth. *Grigné and Labrosse* [2001] proposed that this problem of "missing heat" could be solved by introducing the thermally insulating effect of continents to slow down mantle cooling. The models in that study were, however, simple, considering perfectly insulating continents and assuming an oceanic heat flux not influenced by the continents. A better quantification of the effect of continents on heat transfer across the mantle is clearly necessary. In particular, in the history of continental growth [e.g., *Collerson and Kamber* 1999], we need to know when

[1] Institut für Geophysik, ETH Zürich, ETH Hönggerberg HPP, Zürich, Switzerland.

[2] Sciences de la Terre, Ecole Normale Supérieure de Lyon, Lyon, France.

0148-0227/07/2005JB004192$09.00

continental size is important for the thermal evolution of the Earth.

[5] *Guillou and Jaupart* [1995] built experimental models to study the effect of continents on mantle dynamics, using fixed rigid lids of finite conductivity to represent continents. They obtained a particular pattern of convection, with a zone of upwelling beneath the continent. In this paper, we construct numerical models of convection using a similar approach: Continents are represented by finitely conducting nondeformable lids, while the oceanic zones are the free isothermal parts of the surface. The mechanical boundary conditions are, however, different: The models by *Guillou and Jaupart* [1995] had rigid boundary conditions on their whole surface, while we impose a no shear stress condition.

[6] The choice of free-slip boundary conditions is made in order to fully isolate the purely thermal effect of a lid of finite conductivity. With rigid boundary conditions on the whole surface or on a part of the model, the upper part of the fluid under the zone where a rigid condition is imposed becomes stagnant, with heat transferred by conduction through this part of the fluid, which increases the effective thickness of the imposed lid and leads to a higher thermal insulation. The total effective thickness of the conductive part in the model, that is to say the imposed solid lid and the stagnant fluid, is not a well constrained parameter, since the thickness of the stagnant part of the fluid is not known a priori. We aim to study purely the insulating effect of the lid and thus made the choice to use free-slip boundary conditions in order to fully control the thickness of the insulating lid. The effects of the mechanical coupling between the fluid and the lid will be addressed in another paper.

[7] We also limit this study to models of moderate aspect ratio. The presence of the lid modifies the pattern of convection in the fluid, generating a large-scale horizontal circulation, with convection cells wider than those obtained with no lid. Experiments in the present paper are carried out in boxes of aspect ratio less than or equal to 4. For the case of a lid partially covering the fluid, the lid is in the center of the model, and two convection cells develop, one in each half of the model. These convective cells are always partially covered by the lid, and there is not enough space in the model for the development of cells that are not covered by the lid. The results obtained for larger boxes will be presented in another paper.

[8] A scaling law for the heat transfer efficiency in such models partially covered by a finite conductivity lid was proposed by *Lenardic and Moresi* [2003], but the effect of the geometry of the flow on the heat transfer efficiency was not addressed in their scaling analysis. In the present study, the aspect ratio of the cells is a parameter on which the heat flux depends explicitly.

[9] After a presentation of the model, a scaling law for convection under a lid covering the entire surface of the model is constructed. Results obtained for a partial lid are presented in section 3, and implications for the Earth are presented in section 4.

2. Model

[10] We construct two-dimensional Cartesian models of convection for an isoviscous fluid under a lid of finite conductivity. A sketch of the model and the notations used is presented in Figure 1. Shear stress free mechanical boundary conditions are applied on the horizontal boundaries of the model, and periodicity is imposed on the vertical walls. Regarding the thermal boundary conditions, a fixed temperature is imposed at the base of the model. The lid, set on top of the fluid, can cover either a part or all of the surface of the fluid. In the former case, a fixed temperature of zero is imposed at the surface of the fluid outside the lid. We impose continuity of heat flux and of temperature at the interface between the fluid and the lid. A fixed temperature of zero is imposed on the top of the lid, as well as on its vertical walls in the case of a partial lid. We denote by d_c the thickness of the lid, k_c its thermal conductivity and a its width. d_c, k_c and a are free parameters, whose effects are explored in a systematical way. For the sake of simplicity, we consider only bottom heated cases and have no internal heating in the models.

[11] For the fluid, we solve the equations of convection for a fluid at infinite Prandtl number, using the code Stag [e.g., *Tackley*, 1993]. We use a regular grid with square cells and 128 cells in the vertical direction, so that our resolution is 512 $\times$ 128 for models of aspect ratio 4. Resolution tests were carried out to compare results obtained with this resolution and those obtained with a 1024 $\times$ 256 grid. At Rayleigh numbers smaller than or equal to 10^7, all studied values with the 512 $\times$ 128 resolution, specifically mean temperature, mean local heat flux below the lid and below the free part of the model and mean heat flux on the whole surface of the model, were within 0.6% of the ones obtained with a 1024 $\times$ 256 grid. For Rayleigh numbers $10^7 < Ra \leq 10^8$, the differences did not exceed 1.4%. A regular grid is also added on top of the grid of the fluid, to model the diffusive heat transfer through the conductive lid. The horizontal resolution in the lid is equal to that within the fluid. The vertical resolution depends on the thickness of the lid, and we choose a number of cells inside the lid so that the vertical resolution within the lid is equal or better than that in the fluid.

[12] The finite conductivity lid imposes a "mixed" condition at its base [*Sparrow et al.*, 1964]. Heat is carried through the lid only by conduction. If the lid is wide enough compared to its thickness, that is to say if lateral transfer of heat can be neglected inside the lid, the equation for the temperature T_c of the lid is

$$\frac{\partial T_c}{\partial t} = \kappa_c \frac{\partial^2 T_c}{\partial z^2}, \qquad (1)$$

where κ_c is the thermal diffusivity of the lid. We denote by T_L the temperature at the interface between the lid and the fluid. For a stationary state with no internal heating, the heat flux through the lid is

$$q_c = -k_c \frac{\partial T_c}{\partial z} = -k_c \frac{T_L}{d_c}, \qquad (2)$$

where $z = 0$ at the surface of the fluid and z is positive downward. The continuity of the heat flux through the

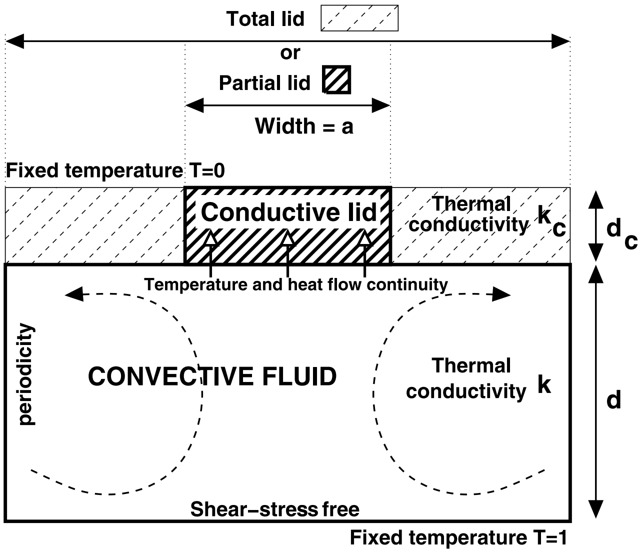

Figure 1. Model and notations used in the present study.

interface between the lid and the fluid leads to the following equilibrium:

$$k\left(\frac{\partial T}{\partial z}\right)_{z=0} = k_c \frac{T_L}{d_c}. \quad (3)$$

Using the depth d of the fluid as the characteristic length, equation (3) gives in a dimensionless form:

$$\left(\frac{\partial T}{\partial z}\right)_{z=0} - \frac{k_c}{k}\frac{d}{d_c}\, T_L = 0. \quad (4)$$

A dimensionless number, named the Biot number [*Sparrow et al.*, 1964], can be introduced:

$$B = \frac{k_c}{k}\frac{d}{d_c}. \quad (5)$$

This number describes the thermal boundary condition seen by the fluid under the lid. If the thermal conductivity k_c of the lid is very low, or if its thickness d_c is large, the Biot number is small. The boundary condition (equation (4)) is then reduced to $(\partial_z T)_0 = 0$, that is to say a condition of fixed zero heat flux. On the other hand, for a thin or very conductive lid, B is large and the controlling term in equation (4) is $T_L = 0$. The thermal boundary condition thus varies from one of fixed heat flux for low values of the Biot number B to one of fixed temperature for large values of B.

[13] To obtain the boundary condition given by equation (4), the hypothesis was made that there is no horizontal transfer of heat within the lid. For a lid of finite width this hypothesis is not accurate, and one must take into account the lateral transfer of heat. This case has been considered by *Hewitt et al.* [1980] and *Guillou and Jaupart* [1995], who showed that the lid is less insulating when significant lateral heat transfer occurs, that is to say for thick lids. Tests were carried out during the present study to quantify the reduction of thermal insulation with thicker lids; the results are presented in the appendix. For the full lid case, the boundary condition is always well described by the externally imposed Biot number. The lateral transfer of heat has a significant effect only for the partial lid cases. In order to be able to quantify the insulating effect of a lid using the Biot number defined a priori using simply k_c and d_c (equation (5)), we chose to carry out experiments with lids whose thickness does not exceed $0.1d$. This value is chosen because horizontal heat diffusion is then almost negligible for the value of the heat flux under the lid. For the numerical implementation, this value is also large enough to allow a significant number of grid points in the lid.

[14] For the Earth, if one assumes the thermal conductivity of the continental lithosphere to be the same as that of the mantle, the Biot number is then the ratio between the thickness of the mantle and that of the continental lithosphere. Using measurements of heat flux in precambrian continental shields in North America and Africa and estimates of concentrations of radioactive elements in the continental crust and subcontinental lithosphere, *Jaupart and Mareschal* [1999] obtained a continental lithosphere thickness of between 200 and 330 km. *Rudnick et al.* [1998], from heat flux measurements and geochemical data in subcontinental xenoliths, gave estimates of continental lithosphere thickness ranging from 150 to 200 km. A new approach was introduced by *Michaut and Jaupart* [2004] using models in which the continental lithosphere is not in steady state, which leads to a nonuniqueness of the solution for the heat flux at the base of the lithosphere and for its thickness, and they obtained possible values of the thickness of between 200 and 270 km for the Kaapvaal craton, South Africa, and the Canadian craton. The range of thickness 150–330 km corresponds to $0.05d < d_c < 0.11d$ for whole mantle convection, and $0.21d < d_c < 0.47d$ for upper mantle convection. This range justifies the choice of $d_c = 0.1\ d$ in numerical experiments for whole mantle convection. It corresponds to $8 < B < 20$ for whole mantle convection and $2 < B < 7$ for upper mantle convection. During this study, experiments were carried out for Biot numbers ranging from 0 to 100.

3. Convection Under a Total Lid

3.1. Patterns of Convection With Insulating Horizontal Boundaries

[15] Laboratory experiments of convection never reach perfect conditions of fixed temperature, and these conditions are only approached using very conductive horizontal walls. The differences that may appear between the case of highly conductive boundaries and the theoretical case of a perfect isothermal condition have thus been studied intensively, in order to understand how laboratory experiments could differ from theoretical studies. However, the case of poorly conductive boundaries has received far less study.

[16] Theoretical studies [*Sparrow et al.*, 1964; *Hurle et al.*, 1967] predicted long wavelengths for convective rolls at the onset of convection when the fluid is bounded by poorly conducting horizontal walls. Possible applications of this for the pattern of convection in the Earth were proposed early on: *Chapman and Proctor* [1980] and *Chapman et al.* [1980] carried out a study of the onset of convection when a heat flux is imposed on the horizontal boundaries of the

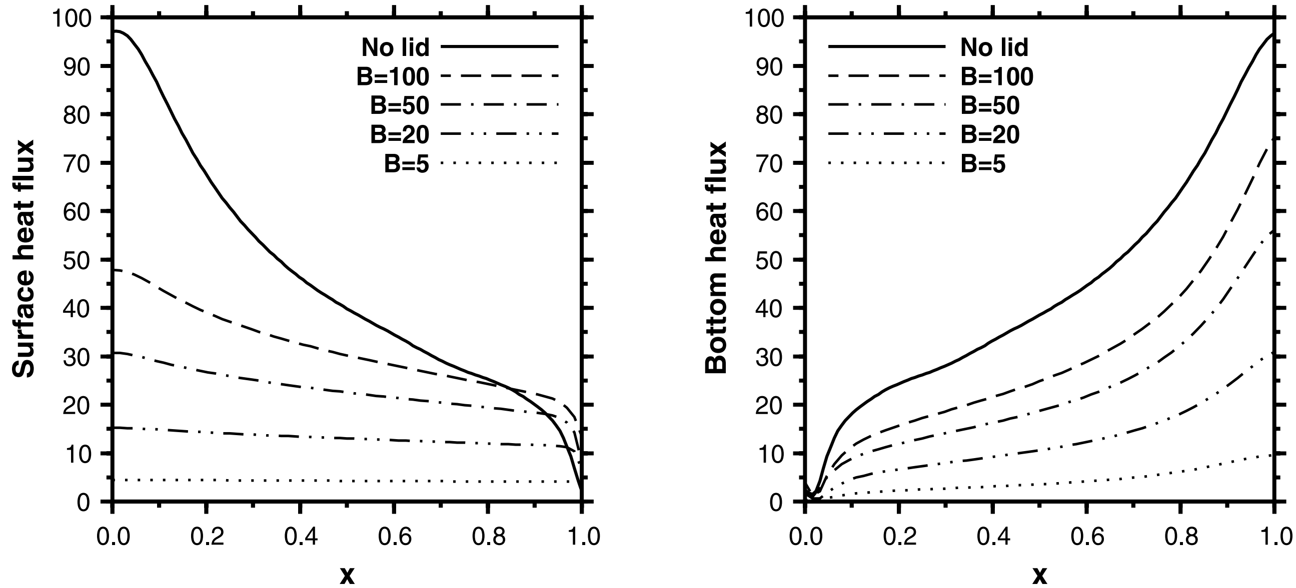

Figure 2. Time-averaged heat flux (left) at the surface of the fluid and (right) at its base, for convection at $Ra = 10^7$ in a model of aspect ratio 2, for isothermal boundary conditions (solid line), or with a lid of finite conductivity at the surface (dashed and dotted lines), for variable Biot numbers. A hot upwelling is located at $x = 0$, and a cold downwelling is located at $x = 1$.

model and showed that short-wavelength modes develop fast but are unstable for all longer wavelength modes, and convective cells then keep on growing with time and are only limited by the dimensions of the model. *Chapman et al.* [1980] then concluded that a boundary condition of fixed heat flux may be more appropriate than a condition of fixed temperature for the Earth. Numerical experiments with fixed heat flux on the two horizontal walls of the fluid were also carried out by *Hewitt et al.* [1980] and they easily obtained convective cells of aspect ratio wider than 5.

[17] These studies all considered symmetrical conditions between the top and the base of the model. The case of nonsymmetrical conditions has received far less attention. One of the rare studies with nonsymmetrical boundaries was carried out by *Ishiwatari et al.* [1994] using a numerical approach. They imposed fixed heat flux or fixed temperature independently at the base and the top of the fluid, with or without internal heating. Experiments were done at $Ra = 10^4$ and with a Prandtl number of 1, which restricts the comparison with the present study for which the Prandtl number is infinite. *Ishiwatari et al.* [1994] obtained a long wavelength of convection only if a fixed heat flux is imposed both at the base and the top of the fluid. *Lenardic and Moresi* [2003] also carried out numerical experiments of convection with a fixed temperature at the base of the fluid and a lid of finite conductivity covering the surface of the model. Unlike in this study, the mechanical boundary conditions were rigid in their experiments. With these asymmetrical conditions and at high Rayleigh numbers larger than 10^7, they obtained convective cells of aspect ratio close to one in models of aspect ratio 4.

[18] In the present study, with a fixed temperature at the base of the fluid, a finitely conducting lid covering the entire surface and free mechanical boundary conditions, we did not obtain a significative increase in the wavelength of convection compared to the case of isothermal boundary conditions: The cells generally have an aspect ratio close to one.

[19] The main difference from the isothermal case concerns the thermal state of the fluid. Under an insulating lid the temperature of the fluid is higher than for isothermal conditions, and for a given Rayleigh number, the mean heat flux is lower. The horizontal profiles of heat flux at the surface and at the base of the fluid are presented in Figure 2, for either isothermal boundary conditions or a finite conductivity lid. With isothermal conditions, the heat flux profiles at the base and at the surface are exactly symmetrical, as expected. With a lid, the horizontal profile of heat flux at the base of the fluid is similar to that without a lid, whereas the heat flux profile at the surface is flatter, with smaller amplitude lateral variations (see Figure 2). Let $q_b^B(x)$ be the heat flux at the bottom of the model for a Biot number B, and $q_b^\infty(x)$ the corresponding quantity for the case of no lid, that is to say $B \rightarrow \infty$. Figure 3 shows that the ratio $q_b^B(x)/q_b^\infty(x)$ is independent of x outside vertical plumes. On the other hand, the ratio $q_t^B(x)/q_t^\infty(x)$ for the heat flux at the surface of the model depends on x, and the flattening of the profile $q_t^B(x)/q_t^\infty(x)$ increases as B decreases, so that for this example at $Ra = 10^7$, the surface heat flux can be considered to be quasi-uniform for Biot numbers smaller than 20 (Figure 2).

3.2. Scaling Law for the Temperature and the Heat Flux Under a Global Lid

[20] When a lid of finite conductivity is set on top of the entire surface of the model, a temperature higher than in the case of an isothermal condition is obtained, as well as a lower mean heat flux for a given Rayleigh number. Examples of

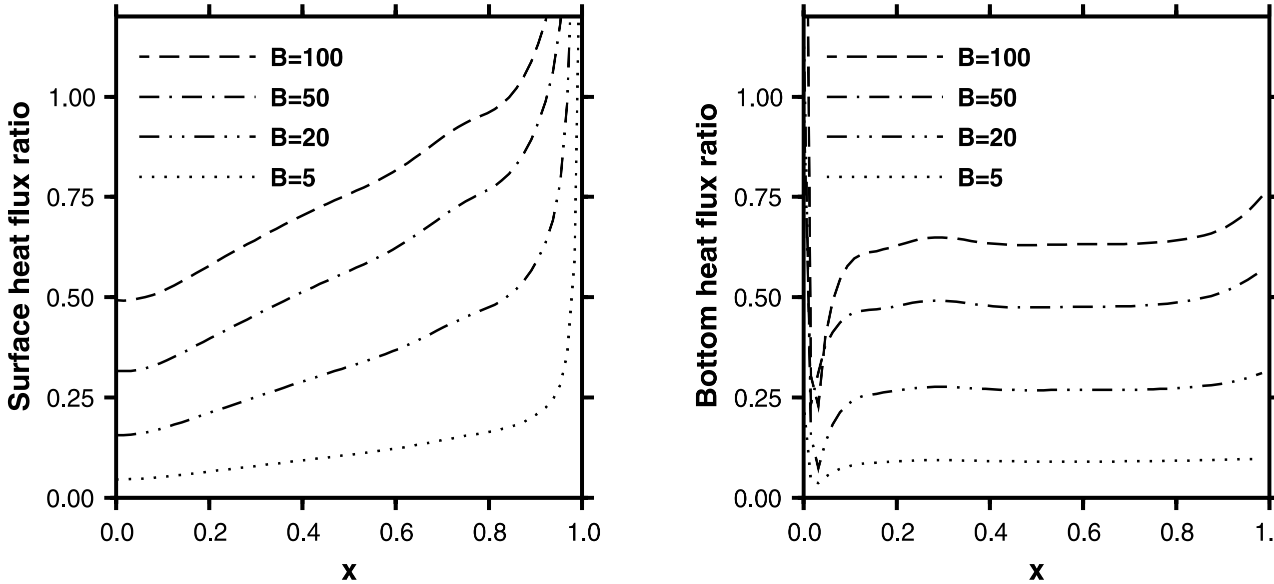

Figure 3. (left) Ratio $q_t^B(x)/q_t^\infty(x)$ and (right) $q_b^B(x)/q_b^\infty(x)$ for the case presented in Figure 2.

vertical profiles of horizontally averaged temperature are presented in Figure 4.

[21] These profiles are classical ones for a convective fluid. Even though the thermal conditions imposed at the base and at the surface of the fluid are not symmetrical any more, the profiles show that the symmetry between the upper and lower boundary layers is maintained, with simply a nonzero temperature at the surface of the fluid. The mean temperature of the fluid for a given Rayleigh number is higher for a smaller Biot number, that is to say for a more insulating lid. For a fixed Biot number, the fluid is hotter at higher Rayleigh number.

[22] T_i is the mean temperature of the fluid, which is also the homogeneous temperature in the core of the convective cells. With symmetrical boundary layers, we can write

$$T_i = \frac{1 + T_L}{2}, \tag{6}$$

where T_L is the temperature at the surface of the fluid. This hypothesis is not perfectly relevant at low Rayleigh numbers ($Ra \leq 10^5$), for which we always obtain a temperature T_L at the interface slightly higher than $2T_i - 1$,

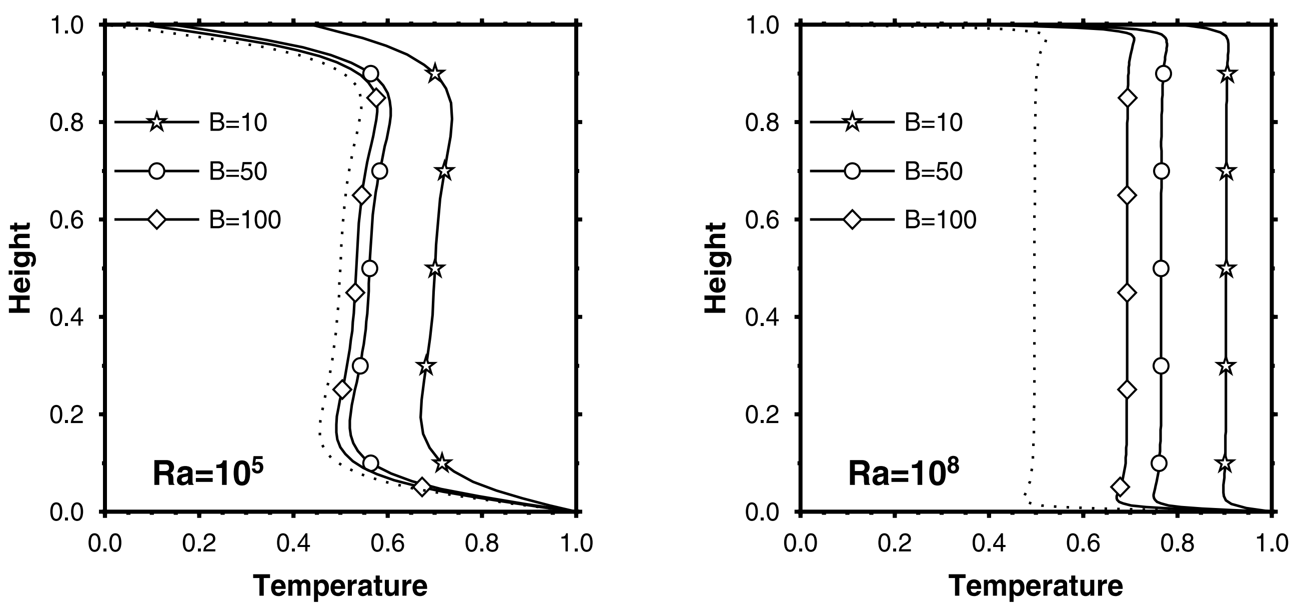

Figure 4. Profiles of horizontally averaged temperature for a convection under a total lid (solid line) or with no lid (dotted line), at $Ra = 10^5$ and $Ra = 10^8$.

but is observed for higher Rayleigh numbers more relevant to the Earth.

[23] When a fixed temperature T_0 is imposed, a boundary layer model can be used, which gives the following mean heat flux [e.g., *Turcotte and Oxburgh*, 1967; *Turcotte and Schubert*, 1982]:

$$q = 2k\ \delta T\left(\frac{u}{\pi\kappa\ell}\right)^{1/2}, \tag{7}$$

where k is the thermal conductivity of the fluid, κ its diffusivity, δT the temperature jump through the thermal boundary layer, and u is the horizontal velocity in the horizontal boundary layers, considered constant and uniform along the width ℓ of the convective cell. At the surface of the fluid, underneath the finitely conducting lid, the heat flux is not of the same form as the flux obtained when a fixed temperature is imposed. Therefore the model given by equation (7) cannot be used. On the other hand, the boundary condition at the base of the fluid is one of fixed temperature, and the heat flux has the form of the one obtained with no lid (see Figures 2 and 3). Equation (7) can thus be used at the base of the fluid. In a dimensionless form, the temperature jump across the lower boundary layer is $1 - T_i$. The characteristic velocity used for the nondimensionalization is the diffusive one: $[u] = \kappa/d$. The dimensionless mean heat flux at the base of the fluid is then

$$Q_b = 2(1 - T_i)\left(\frac{U}{\pi L}\right)^{1/2}, \tag{8}$$

where L is the dimensionless width of the convective cell ($L = \ell/d$). The form of the observed horizontal velocity profiles in the boundary layers stays broadly the same as in experiments with no lid, and the horizontal velocity is the same in the upper and lower boundary layers. We then use the same loop model as the one introduced in *Grigné et al.* [2005], with the same forms for the horizontal profiles of vertical and horizontal velocities. *Grigné et al.* [2005] showed that the form of the vertical velocity at middepth of a convective cell was not linear but that the width on which the vertical velocity is not negligible was always close to the half depth of the model, and we denoted this width by λ. The horizontal velocity u can then be written

$$u = \frac{\kappa}{d}\left(\frac{Ra}{2\sqrt{\pi}}\right)^{2/3}\left(\frac{\delta T}{\Delta T}\right)^{2/3}\frac{(\ell/d)^{1/3}}{\left(\frac{\ell}{d} + \frac{d^3}{8\lambda^3}\right)^{2/3}}, \tag{9}$$

with $\lambda \simeq 0.5\ d$, where d is the depth of the fluid. δT is the temperature difference across the thermal boundary layer. ΔT is the temperature difference between the base of the fluid and the surface of the lid. This difference ΔT is used as the characteristic temperature to render equation (9) nondimensional. The characteristic length is the depth d of the fluid. We thus obtain for the dimensionless velocity U:

$$U = \left(\frac{Ra}{2\sqrt{\pi}}\right)^{2/3}(1 - T_i)^{2/3}\frac{L}{\left(L^2 + \frac{L}{8\lambda^3}\right)^{2/3}}. \tag{10}$$

Equations (8) and (10) then lead to the following mean heat flux at the base of the model:

$$Q_b = \left(\frac{2}{\pi}\right)^{2/3} Ra^{1/3}\ \frac{(1 - T_i)^{4/3}}{\left(L^2 + \frac{L}{8\lambda^3}\right)^{1/3}}. \tag{11}$$

Equation (4), using equation (6) to replace T_L by T_i, can be written

$$Q_t = B(2T_i - 1), \tag{12}$$

where Q_t is the mean heat flux at the surface of the model. The equilibrium between Q_t and Q_b yields

$$\frac{(1 - T_i)^4}{(2T_i - 1)^3} = \frac{B^3}{Ra}\frac{\pi^2}{4}\left(L^2 + \frac{L}{8\lambda^3}\right). \tag{13}$$

We thus obtain a scaling for the mean temperature T_i of the fluid as a function of the Rayleigh number Ra, the Biot number B and the width L of the convective cells. Knowing T_i, the mean heat flux can be obtained using equation (12). The Rayleigh number Ra is here defined using the temperature jump ΔT between the bottom of the fluid and the top of the lid, and thus does not describe exactly the vigor of the convection in the fluid. The effective temperature jump across the fluid is not known a priori, but depends on the Biot number B. The effective Rayleigh number $Ra_{\mathrm{eff}} = Ra\ (1 - T_L)$ for the fluid can thus be computed only a posteriori.

[24] Figure 5 presents the scaling law given by equations (12) and (13) for the temperature T_i and for the mean heat flux compared to the values obtained by the full computation of the equations of convection, and a very good agreement is obtained. One can, however, notice that the predicted heat flux is slightly too low at $Ra = 10^5$. To compute the heat flux, we use $Q_t = B(2T_i - 1)$. This expression depends on the hypothesis $T_L = 2T_i - 1$ (equation (6)), which is not perfectly correct at low Rayleigh numbers, for which we observe $T_L > 2T_i - 1$, yielding a predicted heat flux that is too low.

4. Convection Under a Partial Lid

4.1. Pattern of Convection

[25] We showed in section 3.1 that no modification of the pattern of convection was obtained, compared to isothermal boundary conditions, when a lid of finite conductivity covers the entire surface of the model. However, putting a partial lid of finite conductivity on a fluid whose surface is otherwise isothermal strongly modifies the pattern of convection: A zone of hot upwelling appears under the lid. This result was already obtained in laboratory experiments by

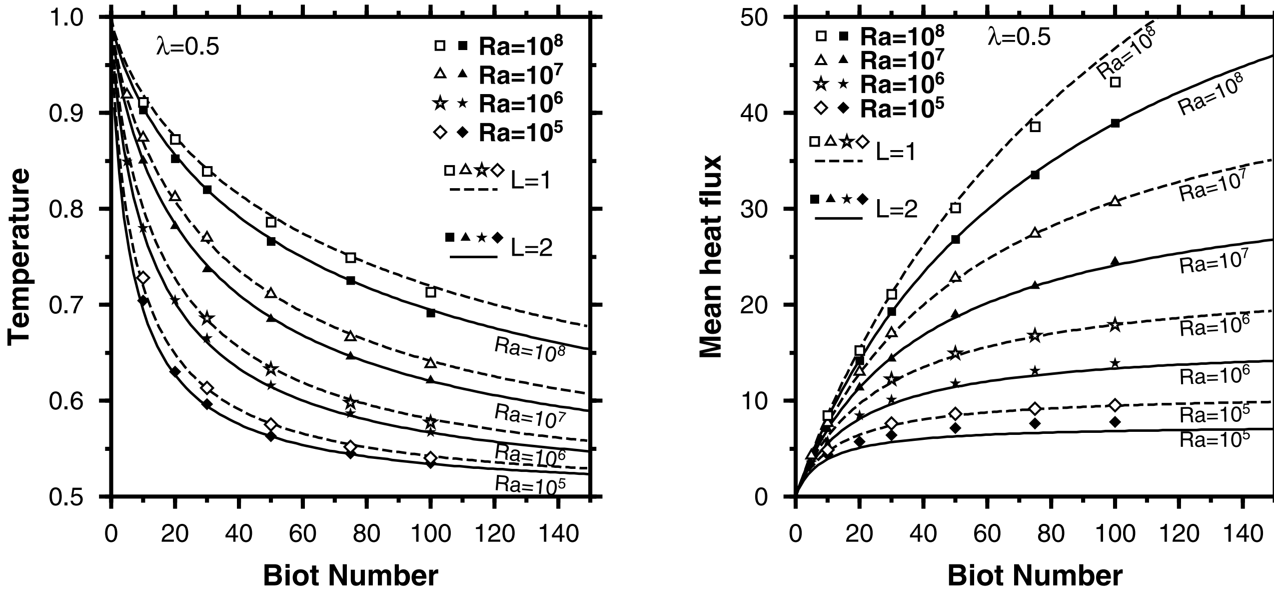

Figure 5. (left) Temperature and (right) mean heat flux as a function of the Biot number, predicted by the scaling law proposed in this paper, compared to the values obtained by numerical models of convection (symbols), for different Rayleigh numbers and for cells of width L = 1 or L = 2, obtained in models of aspect ratio 2 and 4, respectively.

Guillou and Jaupart [1995] and in numerical experiments that include insulating continents [e.g., *Gurnis*, 1988; *Gurnis and Zhong*, 1991; *Lowman and Jarvis*, 1993; *Zhong and Gurnis*, 1994; *Trubitsyn and Rykov*, 1995; *Bobrov et al.*, 1999; *Lowman and Gable*, 1999; *Yoshida et al.*, 1999; *Honda et al.*, 2000]. Figure 6 presents the temperature fields obtained for two values of the Rayleigh number under a lid with a Biot number $B = 10$. At $Ra = 10^5$ convection is stationary with a fixed hot plume centered under the lid. At higher Rayleigh numbers convection is time-dependent and exhibits a set of small plumes under the lid.

4.2. Two Regimes of Cellular Circulation

[26] In the rest of this paper, two regimes of cellular circulation will be described: The first one, named "free loop," is the one obtained when sets of hot and cold plumes are present on wide zones of the model (e.g., the case $Ra = 10^8$ in Figure 6). The second one, named "forced loop," is obtained when the circulation can be described as real convective cells (e.g., $Ra = 10^5$ in Figure 6). The difference and transition between these two regimes is presented hereafter.

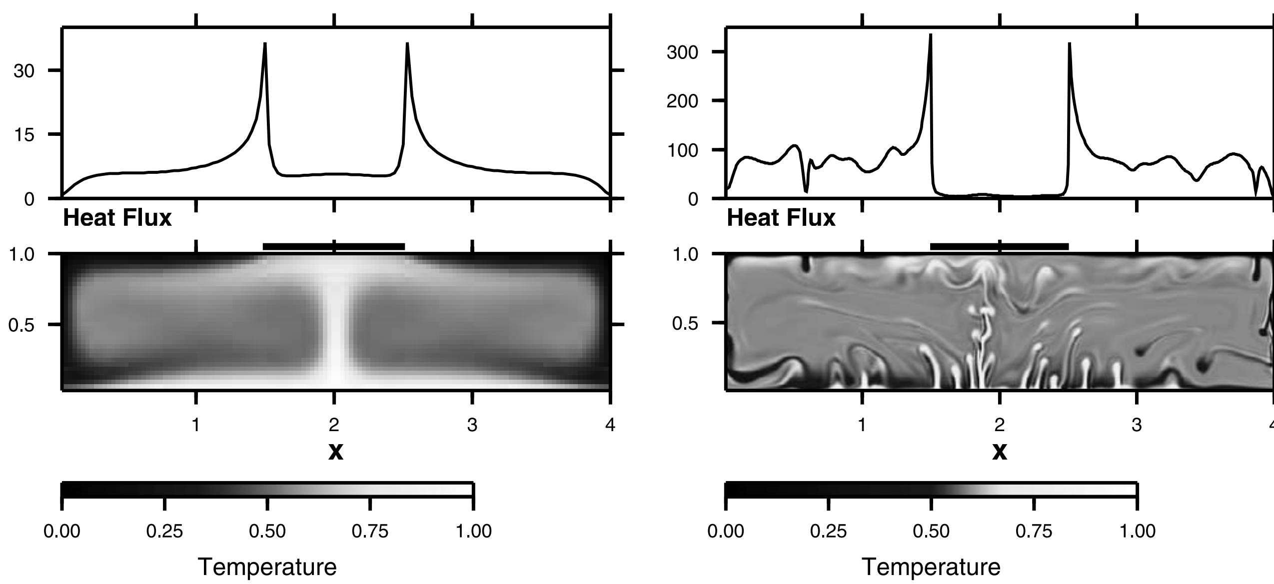

Figure 6. Temperature fields obtained under a lid with a Biot number $B = 10$ at Rayleigh numbers (left) 10^5 and (right) 10^8. The case in Figure 6 (left) is in the forced loop regime, and the one in Figure 6 (right) is in the free loop regime (see text for explanations).

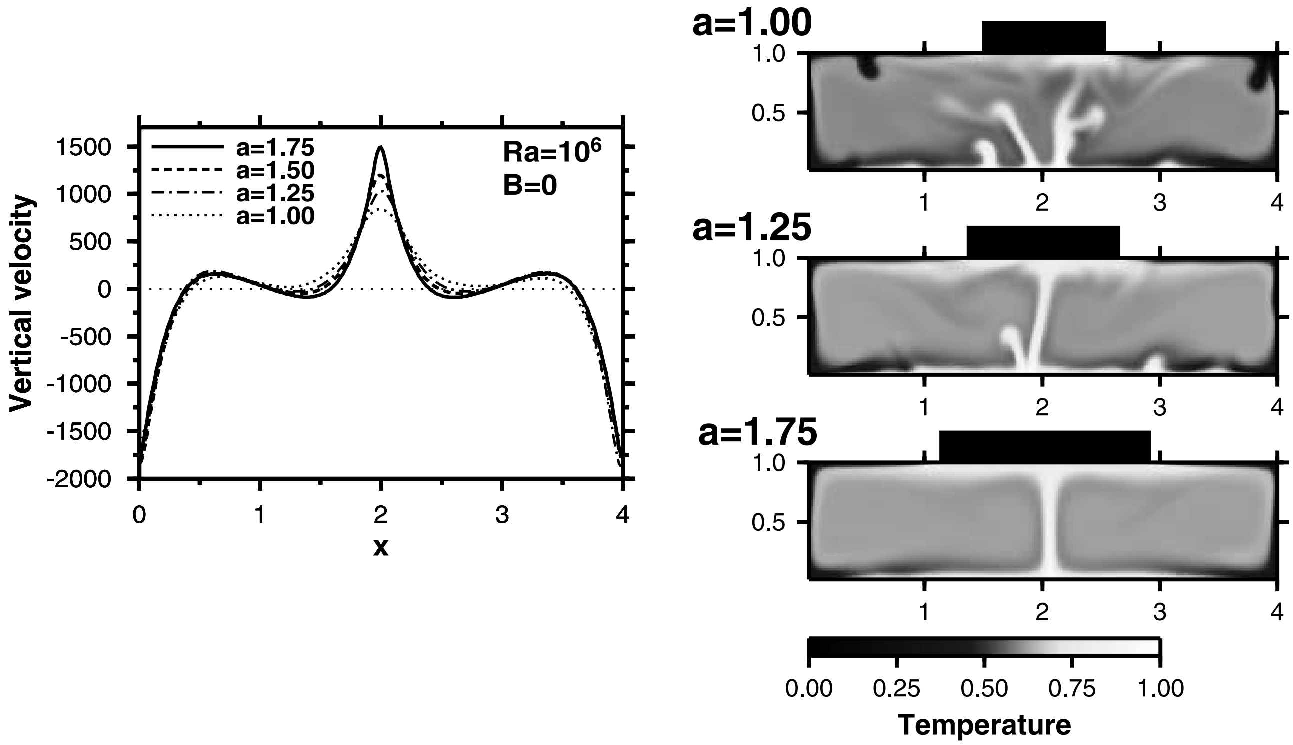

Figure 7. (left) Horizontal profiles of temporally averaged vertical velocity at middepth at $Ra = 10^6$ under a perfectly insulating continent of variable width and (right) snapshots of the corresponding temperature fields. The transition from free to forced loop regime as the continental size increases is illustrated.

[27] Figure 7 presents the horizontal profiles of temporally averaged velocity at middepth for $Ra = 10^6$ and $B = 0$ for a model of aspect ratio 4, for lid width ranging from 1.0 to 1.75, as well as snapshots of the corresponding temperature fields. For $a = 1$ there is a clear contrast between the vertical velocity of the hot and cold plumes. For wider lids, the velocity of the hot plume under the lid increases gradually and becomes equal to that of the cold plume for $a = 1.75$. Figure 7 (right) shows that this evolution corresponds to the transition between an upwelling with several small plumes and an upwelling with a single hot plume under the center of lid. We thus observe a transition between two regimes when the width of the lid is increased.

[28] The regime that was named free loop is obtained for narrow lids, and the forced loop regime is obtained for wide lids, or for low Rayleigh numbers for which convection is stationary. In the former regime, the lid is narrow enough for the upper boundary layer, under the fixed temperature zone, to cool and reach the threshold thickness for cold plumes to form before the vertical boundary of the model is encountered. For the latter, the lid is too wide compared to the size of the model to let a free cellular circulation develop, and the convection pattern is forced by the size of the model. These two regimes are shown schematically in Figure 8.

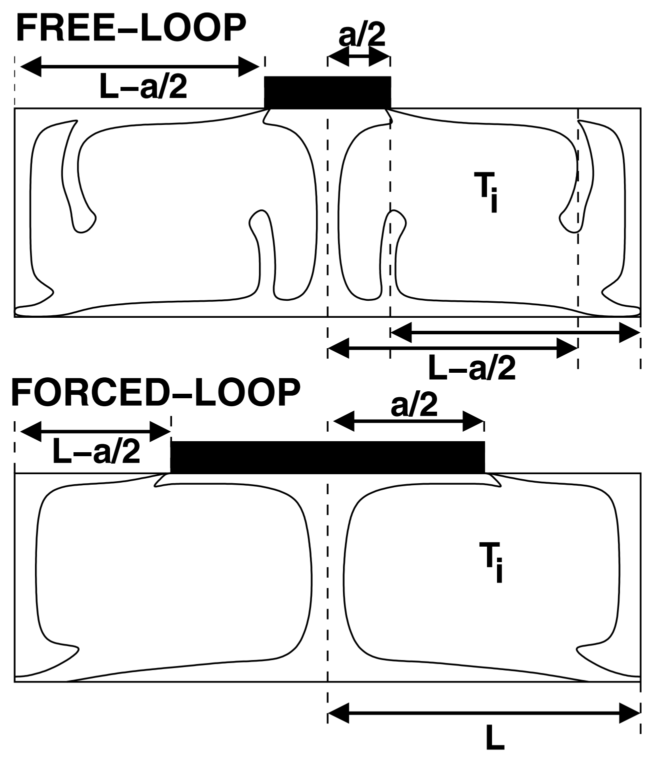

Figure 8. Schemes of the two regimes of cellular circulation under a lid.

5. Scaling Laws

[29] To construct a scaling law for the heat flux out of the model, four parameters have to be considered: the width of

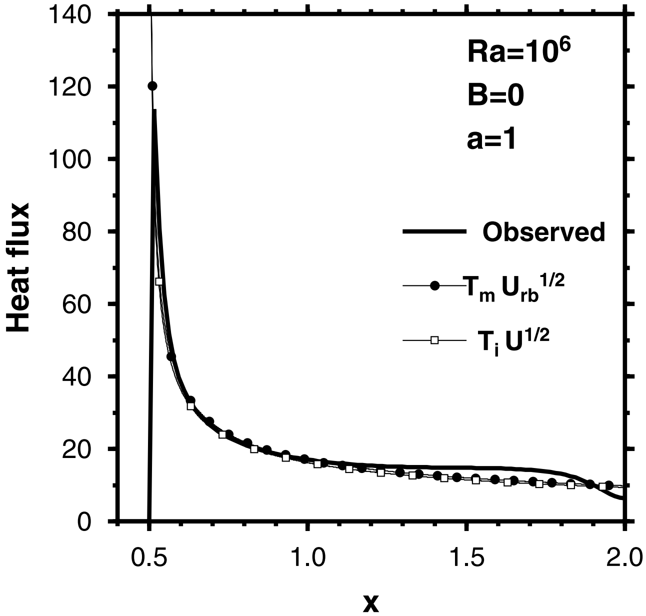

Figure 9. Observed time-averaged surface heat flux with the center of the continent located in $x = 0$, for a continent of width 1 (edge of the continent at the position $x = 0.5$). Solid circles indicate the model given by equation (14), and open squares indicate the model given by equation (16).

the model, the width of the lid, the Biot number, and the Rayleigh number of the fluid. For simplicity, we will first consider the case of a perfectly insulating lid ($B = 0$). To simplify the writing, we will also refer to the lid as "continent," and to the zone outside the lid as "ocean", and the fluid will be named "mantle." We remain, however, aware of the simplicity of the model, and one must keep in mind the fact that we study an isoviscous fluid under a nondeformable lid of finite conductivity.

5.1. Zero Heat Flux Under the Continent

5.1.1. Heat Flux Scaling

[30] For the oceanic part of the surface, we can use a model of cooling by conduction of a half-space, and with a perfectly insulating continent, we can consider that the upper boundary layer starts to cool and thicken only beyond the edge of the continent. Using a system of reference such that $x = 0$ is the position of the center of the continent, the edge of the continent is located at $x = a/2$ and the oceanic heat flux in a dimensionless form can be written

$$q_{oc}(x) = \Delta T_{oc}\left(\frac{U}{\pi(x - a/2)}\right)^{1/2}, \tag{14}$$

where U is the mean horizontal velocity at the surface and ΔT_{oc} is the temperature jump across the thermal boundary layer. We observe in our models that the mantle is thermally well mixed in the core of the convective cell, and T_i denote this homogeneous temperature. The temperature jump ΔT_{oc} is then

$$\Delta T_{oc} = T_i. \tag{15}$$

We observe that the horizontal velocity U is reduced compared to the case of simple Rayleigh-Bénard convection with no continent. The profiles of horizontally averaged temperature in models with a partial continent have a form similar to what is obtained with a full continent, shown in Figure 4, with temperature jumps that are equal through the upper and bottom thermal boundary layers. The total dimensionless temperature jump across the mantle is therefore not $\Delta T = 1$, as would be obtained with no continent, but $\Delta T = 2\,(1 - T_i)$. The insulating effect of the continent gives a temperature T_i greater than 0.5, so that $\Delta T < 1$. This decreased temperature jump across the model explains the observed reduced velocity, but the relationship is not straightforward: The high temperature T_i implies that the buoyancy available to drive hot upwellings is reduced compared to the case with no continent, but there is more buoyancy available for cold downwellings. These two opposite effects lead to a velocity U which is not a simple function of the temperature jump $1 - T_i$.

[31] However, we observe empirically that the values of the temperature T_i and the mean velocity U are always coupled in such a way that the observed heat flux $q_{oc}(x)$ over the oceanic part of the model is very close to the heat flux that would come out of a normal convective cell of width L, with a mean temperature $T_m = 0.5$ and with the upper boundary layer starting to cool at the position $x = a/2$, that is to say

$$q_{oc}(x) = T_m\left(\frac{U_{rb}}{\pi(x - a/2)}\right)^{1/2}, \tag{16}$$

where U_{rb} is the horizontal velocity for simple Rayleigh-Bénard convection for a convective cell of width L. This velocity is [*Grigné et al.*, 2005]

$$U_{rb} = \left(\frac{Ra}{2\sqrt{\pi}}\right)^{2/3} T_m^{2/3} \frac{L}{\left(L^2 + \frac{L}{8\lambda^3}\right)^{2/3}}, \tag{17}$$

where $\lambda \simeq 0.5$.

[32] An example is shown in Figure 9, for $Ra = 10^6$, a continent of width $a = 1$ and a convective cell of width $L = 2$. The observed time-averaged heat flux is presented, as well as the models given by equations (14) and (16), showing that these two models equally well fit the observed heat flux.

[33] Equations (14) and (16) give for the horizontal velocity:

$$U = U_{rb}\left(\frac{T_m}{T_i}\right)^2. \tag{18}$$

The mean horizontal velocities obtained in models with different Rayleigh numbers and continental widths are presented in Figure 10 as a function of the internal temperature T_i, along with the model given by equation (18), and it shows a good agreement.

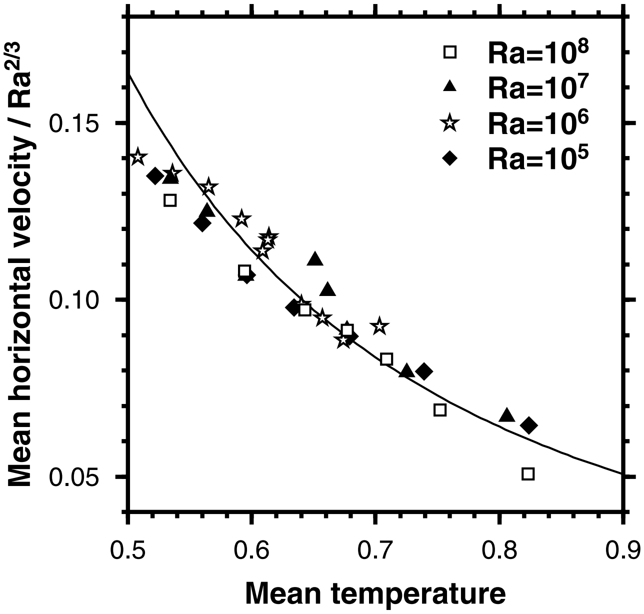

Figure 10. Observed time-averaged horizontal velocity at the surface of models of aspect ratio 4, as a function of the mean temperature T_i, for different Rayleigh numbers (symbols) and for different widths of the continent. The solid line is the model given by equation (18).

[34] From equation (16), we can derive the mean heat flux over the oceanic part of the model:

$$Q_{oc} = \frac{1}{L - a/2} \int_{a/2}^{L} T_m \left(\frac{U_{rb}}{\pi(x - a/2)} \right)^{1/2} dx = 2\ T_m \left(\frac{U_{rb}}{\pi(L - a/2)} \right)^{1/2}. \tag{19}$$

With U_{rb} given by equation (17), we obtain

$$Q_{oc} = \left(\frac{2}{\pi} \right)^{2/3} Ra^{1/3} \frac{T_m^{4/3}}{\left(L^2 + \frac{L}{8\lambda^3} \right)^{1/3}} \left(\frac{L}{L - a/2} \right)^{1/2}. \tag{20}$$

The heat balance in the mantle for the case of a perfectly insulating continent is

$$\left(L - \frac{a}{2} \right) Q_{oc} = L\ Q_b, \tag{21}$$

so that the mean heat flux at the base of the model is

$$Q_b = \left(\frac{2}{\pi} \right)^{2/3} Ra^{1/3} \frac{T_m^{4/3}}{\left(L^2 + \frac{L}{8\lambda^3} \right)^{1/3}} \left(\frac{L - a/2}{L} \right)^{1/2}, \tag{22}$$

which is simply the mean heat flux obtained for Rayleigh-Bénard convection, multiplied by $(1 - a/(2L))^{1/2}$. This model is presented with solid lines in Figure 11 and nicely predicts the observed heat flux.

5.1.2. Temperature

[35] For a global lid with a fixed Biot number, the mean temperature of the fluid is higher for a higher Rayleigh number (see Figure 5). This trend is much less obvious for a partial lid, especially for highly insulating lids. Temperatures obtained for a perfectly insulating lid for various Rayleigh numbers and various widths of the lid are presented in Figure 12.

[36] The form of the mean temperature T_i as a function of the lid width a is relatively complex. One can for instance study the form of T_i as a function of a for the case $Ra = 10^6$ (stars in Figure 12): T_i first increases linearly with a, up to $a = 1$, and then stays broadly constant up to $a = 1.75$, before it increases again. The same behavior is observed for $Ra = 10^7$ (triangles), but with a plateau observed for $1.5 < a < 2$. The trend $T_i = f(a)$ is more monotonic for $Ra = 10^5$ and $Ra = 10^8$. These trends can be associated with the two regimes of cellular circulation defined in section 4.2.

[37] For $Ra = 10^6$, the transition between the two regimes of cellular circulation for a going from 1.0 to 1.75 (see Figure 7) corresponds exactly to the plateau in the temperature increase. The same behavior is observed for $Ra = 10^7$, but for a going from 1 to 2. For $Ra = 10^5$ the convection is always steady state, whatever the continental width. In contrast, for $Ra = 10^8$ there are always several hot plumes under the continent. These two last cases thus have a more continuous trend than the ones where there is a clear transition between the two flow regimes (Figure 12).

[38] From the global heat balance we already obtained a scaling law for the heat flow at the base of the model (equation (22)). To get a scaling for the temperature in the model, we can compare that expression to another, independent expression, obtained by noting that the form of this

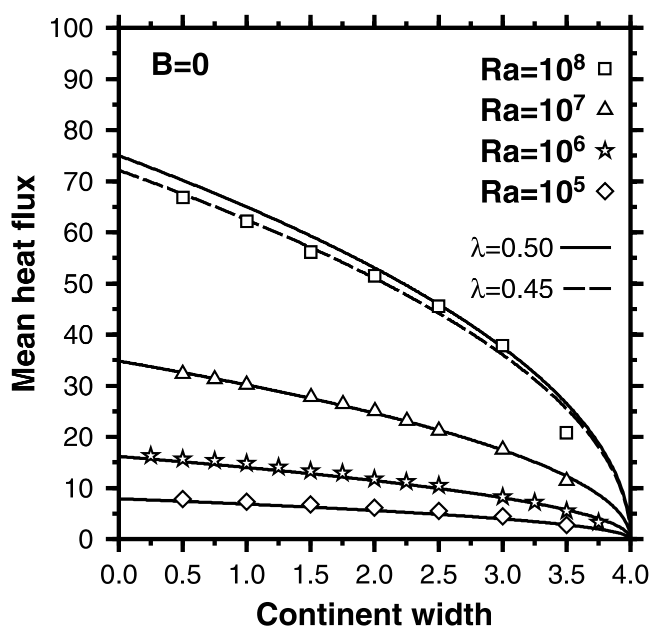

Figure 11. Mean heat flux at the base of models of aspect ratio 4, under a perfectly insulating continent of variable width. Solid lines correspond to the model given by equation (22).

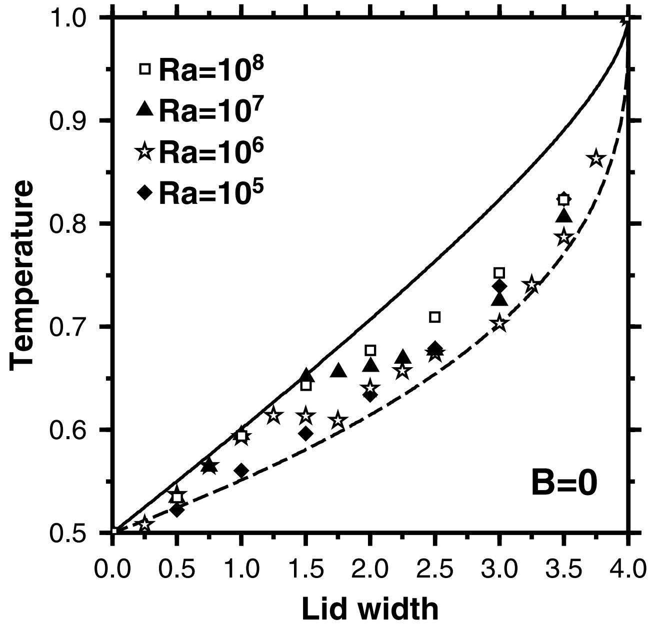

Figure 12. Mean temperature of the fluid for various Rayleigh numbers as a function of the continental width for a model of aspect ratio 4. The continent is perfectly insulating. The solid line is obtained for the free loop model (equation (26)), and the dashed line is obtained for the forced loop model (equation (25)).

flux is similar to the one obtained in a normal Rayleigh-Bénard convective cell, as was the case for a lid covering the whole surface of the model (see Figures 2 and 3 and section 3.1). The temperature jump to be considered at the base of the mantle is $1 - T_i$, so that the mean heat flux at the base of the model for a cell of width L should be written

$$Q_b = \left(\frac{2}{\pi}\right)^{2/3} Ra^{1/3} \frac{(1 - T_i)^{4/3}}{\left(L^2 + \frac{L}{8\lambda^3}\right)^{1/3}}. \qquad (23)$$

However, the hypothesis that the heat flux at the base of the model corresponds to a cell of width L is verified only for the regime named forced loop, where the convective cell actually spreads over the whole width L of the model. For the free loop regime, with a cellular circulation consisting of a set of small plumes, one can consider as a first approximation that for each hot plume, there is a corresponding cold plume at a distance $L - a/2$ (Figure 8). Hence the mean heat flux at the base of the model is not the one given by equation (23) but instead

$$Q_b = \left(\frac{2}{\pi}\right)^{2/3} Ra^{1/3} \frac{(1 - T_i)^{4/3}}{\left((L - a/2)^2 + \frac{L-a/2}{8\lambda^3}\right)^{1/3}}. \qquad (24)$$

[39] For the forced loop regime, equations (22) and (23) give, for the mean temperature T_i,

$$T_i = 1 - T_m \left(\frac{L - a/2}{L}\right)^{3/8}, \qquad (25)$$

and for the free loop regime, equations (22) and (24) yield

$$T_i = 1 - T_m \left(\frac{L - a/2}{L}\right)^{3/8} \left(\frac{(L - a/2)^2 + \frac{L-a/2}{8\lambda^3}}{L^2 + \frac{L}{8\lambda^3}}\right)^{1/4}. \qquad (26)$$

These two models are presented in Figure 12. The observed temperatures almost all lie within the limits of these two models. The free loop model is valid for narrow continents for $Ra \geq 10^6$, and values tend toward the forced loop model for larger continents.

5.2. Nonzero Heat Flux Under the Continent

[40] We first consider the case of an imposed heat flux under the continent, and denote this heat flux by Q_c. Figure 13 shows that the mean oceanic heat flux decreases linearly for increasing imposed continental heat flux for continents of a given width. The slope α in the linear relation between Q_{oc} and Q_c depends on the width a of the continent:

$$Q_{oc} = Q_{oc}^0 - \alpha(a)\, Q_c, \qquad (27)$$

where Q_{oc}^0 is the mean oceanic heat flux obtained for a perfectly insulating continent ($Q_c = 0$) of width a.

[41] To find the expression for the slope $\alpha(a)$, we assume that equation (27) is still valid in the extreme case where the continent is not insulating at all, that is to say in the case where the mean heat flux under the continent is what would

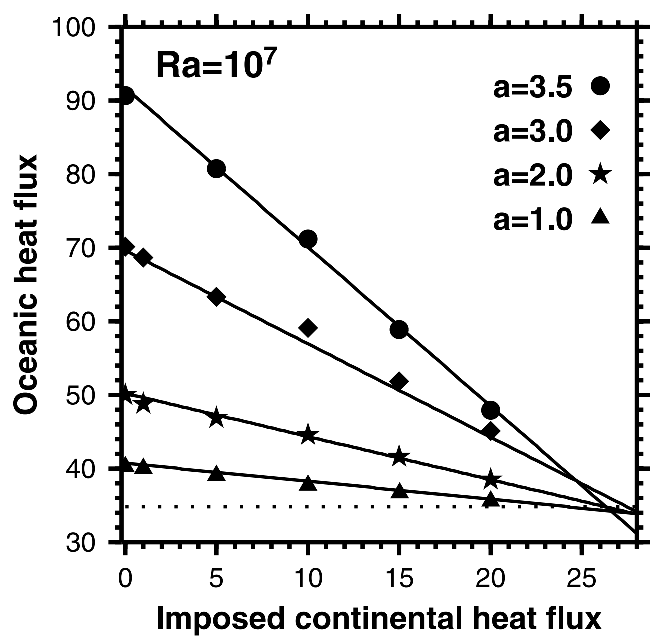

Figure 13. Mean oceanic heat flux as a function of the imposed heat flux under the continent for models of aspect ratio 4, at $Ra = 10^7$. Symbols are the observed values. Straight lines have the slope given by equation (32); a is the width of the continent. The heat flux given by the dotted line is the one obtained without continent.

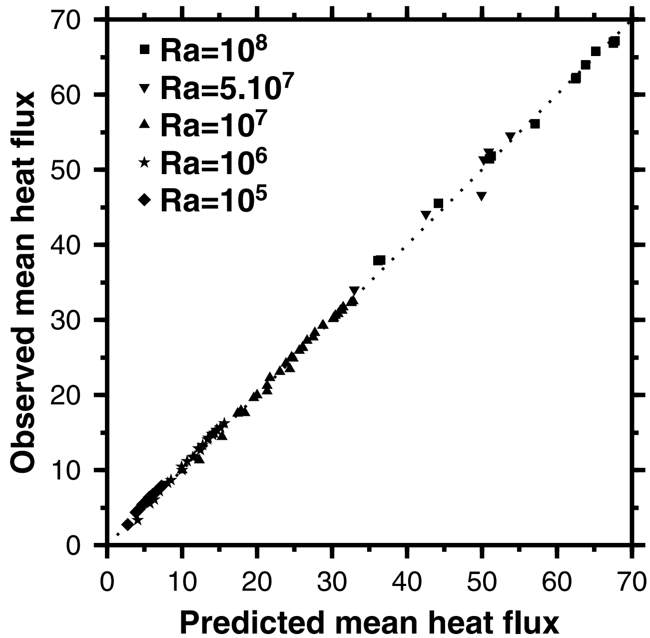

Figure 14. Mean heat flux obtained in models with an imposed fixed heat flux under the continent, as a function of the heat flux predicted by equation (35). Results are obtained for models of aspect ratio between 2 and 6 and Rayleigh numbers $10^5 < Ra < 10^8$.

be obtained over the same zone with no continent. Using the following form for the surface heat flux:

$$q(x) = T_m \left(\frac{U_{rb}}{\pi x}\right)^{1/2}, \tag{28}$$

we compute this heat flux Q_{cz} under the continental zone:

$$Q_{cz} = \frac{2}{a}\int_0^{a/2} T_m \left(\frac{U_{rb}}{\pi x}\right)^{1/2} dx = 2\ T_m \left(\frac{2U_{rb}}{\pi a}\right)^{1/2}. \tag{29}$$

The same computation can be done for the oceanic zone between $x = a/2$ and $x = L$:

$$\begin{aligned} Q_{oz} &= \frac{1}{L - a/2}\int_{a/2}^{L} T_m \left(\frac{U_{rb}}{\pi x}\right)^{1/2} dx \\ &= 2\ T_m \left(\frac{U_{rb}}{\pi}\right)^{1/2} \left(\frac{L^{1/2} - (a/2)^{1/2}}{L - a/2}\right). \end{aligned} \tag{30}$$

For a perfectly insulating continent, the cooling of the upper thermal boundary layer starts after the continental zone, at $x = a/2$, and the mean oceanic heat flux Q^0_{oc} is given by equation (19). In order for equation (27) to still be valid when no continent is present, the following equation must be correct:

$$Q_{oz} = Q^0_{oc} - \alpha(a)\, Q_{cz}. \tag{31}$$

[42] Taking Q^0_{oc}, Q_{cz}, and Q_{oz} from equations (19), (29) and (30), respectively, we obtain the slope $\alpha(a)$:

$$\alpha(a) = \frac{(a/2)^{1/2}}{L - a/2}\left[(L - a/2)^{1/2} - L^{1/2} + (a/2)^{1/2}\right]. \tag{32}$$

These coefficients $\alpha(a)$ have been used to plot the solid lines in Figure 13. The energy conservation in the mantle is

$$L\ Q_b = \left(L - \frac{a}{2}\right) Q_{oc} + \frac{a}{2} Q_c. \tag{33}$$

Q_{oc} is given by equation (27), with $\alpha(a)$ given by equation (32) and Q^0_{oc} by equation (19), which can also be written

$$Q^0_{oc} = Q_{rb}\left(\frac{L}{L - a/2}\right)^{1/2}, \tag{34}$$

where Q_{rb} is the mean heat flux obtained for simple Rayleigh-Bénard convection for a cell of width L. This leads to the following expression for the mean heat flux at the base of the mantle, when a fixed heat flux Q_c is imposed under the continent:

$$Q_b = \left(\frac{L - a/2}{L}\right)^{1/2} Q_{rb} + \frac{(a/2)^{1/2}}{L}\left(L^{1/2} - (L - a/2)^{1/2}\right) Q_c. \tag{35}$$

[43] All the results obtained during the present study with an imposed continental heat flux are plotted in Figure 14 and indicate a very good agreement between the scaling law given by equation (35) and the heat flux observed in full models of convection.

[44] To extend this scaling law to the case of a continental lid of finite conductivity with a given thickness, we use, for the heat flux Q_c under the continent, the flux that is obtained for the case of a continental lid covering the whole surface of the model. There is no algebraic solution for this heat flux under a total lid, as shown in section 3.2, and we use equations (12) and (13) to get the heat flux under the continent. The mean heat flux can then be computed as a function of the Rayleigh number of the mantle, the width of the convective cell L, the Biot number B and the width a of the continent.

[45] The comparison between this scaling law and the observed values of the mean heat flux in two-dimensional models of convection is presented in Figure 15, which shows that our scaling nicely predicts the observed values of the heat flux. However, the simplification that consists of using the scaling law obtained for a total lid in the case of a partial continent is accurate only for low Biot numbers, that is to say for a continent with a significant insulating effect, and for large enough continents. In those cases only, the observed heat flux under a partial lid is close to that obtained for a total lid. Figure 15 indicates a poor agreement between our scaling law and the observed heat flux at $Ra = 10^5$ for Biot numbers $B = 100$ and $B = 20$. The prediction is also unsatisfactory at $Ra = 10^6$ for $B = 100$.

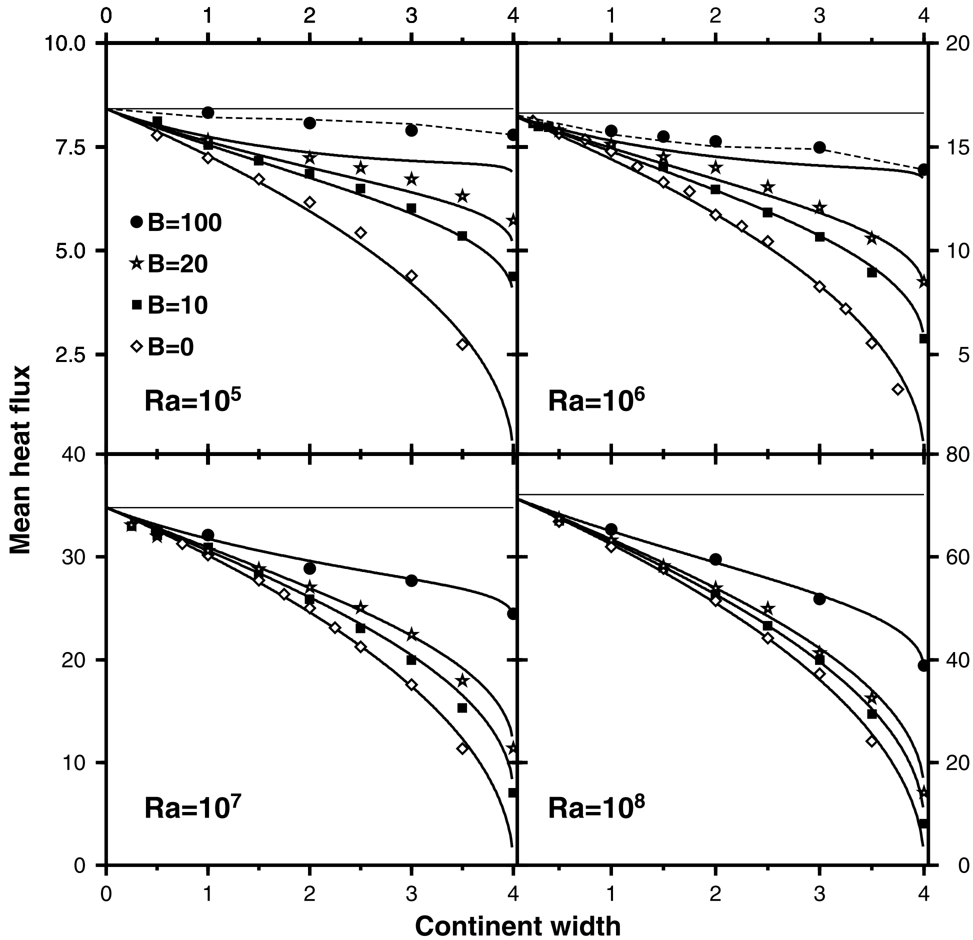

Figure 15. Mean heat flux obtained in models of aspect ratio 4 with a partial lid. Symbols are the observed values for different Biot numbers. The thin horizontal lines give the heat flux obtained with no continent. The thick solid lines are obtained with the scaling law given by equation (35), using for Q_c the continental heat flux calculated with the scaling law proposed for a continental lid covering all the surface of the model (equations (12) and (13)). The dashed lines at Ra = 10^5 and Ra = 10^6 are obtained using the scaling law given by equation (35) but with the actual observed heat flux under the continent for Q_c.

[46] These discrepancies can be understood by going back to the significance of the Biot number. The Biot number represents the maximum heat flux that can be lost through the continent. Indeed, if no heat is lost laterally inside the lid, the boundary condition at the surface of the mantle under the continent is written $(\partial_z T)_{z=0} = B\ T_L$. The temperature T_L at the interface between the continent and the mantle cannot be larger than 1, and the Biot number is thus the maximum dimensionless heat flux $(\partial_z T)_{z=0}$ under the continental lid. A comparison between this value and the heat flux obtained at a given Rayleigh number with no continent gives a good insight of the insulating efficiency of a continental lid. At Ra = 10^5 and Ra = 10^6, the dimensionless heat flux obtained for convective cells of width $L = 2$ with no continent is 8.42 and 16.6, respectively. A continent of Biot number $B \geq 20$ then has a low thermal blanketing effect at both these Rayleigh numbers. The heat fluxes obtained under the partial continent for the cases presented in Figure 15 are then significantly larger than the ones predicted in the case of a full lid, which renders the method used here inaccurate. The scaling law given by equation (35), using the actual observed continental heat flux for Q_c instead of the scaling law given in section 3.2, is plotted with dashed lines in Figure 15 for the cases B = 100 at Ra = 10^5 and Ra = 10^6. This shows that the discrepancy between the parameterization and the observed heat flux at low Rayleigh numbers is due to the simplification that we made, consisting of using the predicted heat flux for a total lid in the case of a partial lid.

[47] Equations (33) and (35) allow the derivation of the mean oceanic heat flux:

$$Q_{oc} = \left(\frac{L}{L-a/2}\right)^{1/2} Q_{rb} - \frac{(a/2)^{1/2}}{L-a/2}\left[(L-a/2)^{1/2} + (a/2)^{1/2} - L^{1/2}\right] Q_c. \quad (36)$$

For the case with Ra = 10^7, Figure 16 presents the mean heat flux in the oceanic and in the continental portions of the model, using equation (36) for the predicted mean oceanic heat flux, and the scaling law given by equations (12)

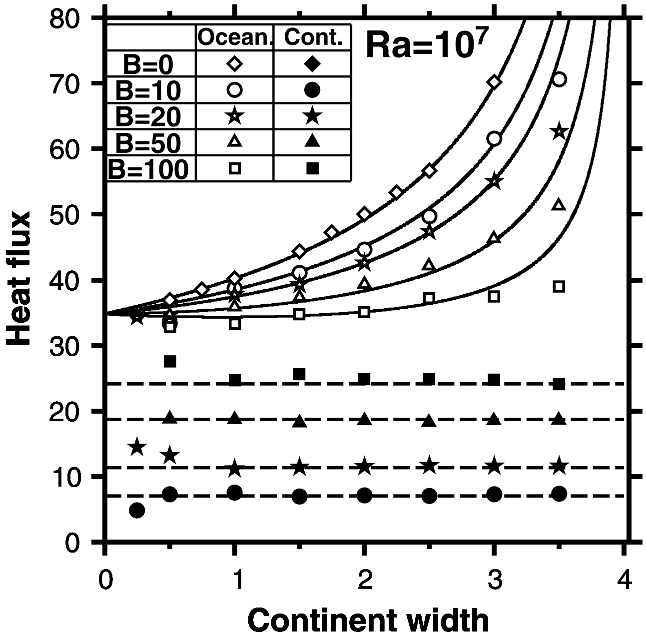

Figure 16. Mean heat flux under the oceanic part of the model, observed (open symbols) and predicted (solid lines) and mean heat flux under the continental part of the model, observed (solid symbols) and predicted (dashed lines), at $Ra = 10^7$.

and (13) to predict the mean continental heat flux. This shows that our theory, with the restriction mentioned above, allows one to derive not only the mean heat flux over the whole surface of the model, but also the local mean flux below the oceanic part of the model and below the continent. The prediction holds for continents that are neither too narrow ($a \leq 0.5$) nor too wide ($a \geq 3.5$). In the former case, lateral transfer of heat within the continental lid cannot be neglected, rendering the effective insulating effect of the continent different from what is predicted with the Biot number defined a priori using only the thickness and thermal conductivity of the lid. In the latter case, the oceanic part of the model is too narrow for our model to be valid: We compute the mean oceanic heat flux using the idea that the cooling of the thermal boundary layer below the oceanic surface of the model starts at the border of the continent. With a wide continent, this hypothesis does not hold, as the cooling of the thermal boundary layer already started below the continent.

[48] No more precise scaling law for the heat flux under a continent covering only a part of the surface of the model could be found during the present study. It is, however, to be noted that the scaling law is satisfactory for the Rayleigh and Biot numbers estimated for the Earth's mantle and the continental lithosphere: We indicated in section 2 that the Biot number for the continental lithosphere for whole mantle convection was lower than 20, which corresponds to a domain of validity of the scaling law for the Rayleigh number: $Ra > 5.10^6$, which is expected for whole mantle convection. Under this restriction, the agreement between the scaling law and the observed values is very good.

[49] The scaling law for a global lid proposed in section 3.2 and the results plotted in Figure 5 indicate that the insulating effect of a lid at a given Biot number is higher at higher Rayleigh number. We noted above that the Biot number is the maximum heat flux that can be observed under the lid. To have a perception of the insulating efficiency of the lid, the Biot number must therefore be compared to the heat flux obtained with no lid at a given Rayleigh number. The fact that a lid with a fixed Biot number is more insulating at higher Rayleigh numbers is also clearly visible in Figure 15. For a continent covering the whole surface of the model, the reduction in the mean heat flux for $B = 100$, compared to what is obtained with no continent, is of 4%, 6%, 17% and 21% for $Ra = 10^5$, 10^6, 10^7 and 10^8, respectively. The lines obtained for the different nonzero Biot numbers tend to get closer to the case $B = 0$ when Ra increases, due simply to the fact that the ratio between the Biot number and the heat flux obtained with no continent decreases with Ra, which renders the effect of the lid closer to that of a perfectly insulating lid with higher Rayleigh numbers.

6. Applications to the Earth

6.1. Insulating Effect of Continents

[50] The experiments carried out during the present study and the scaling laws obtained for the cases of a total or partial lid show that the insulating effect of a lid of finite conductivity is stronger at higher Rayleigh numbers. This effect leads to a lower mean heat flux over the whole surface of the model compared to a convection with no lid at the same Rayleigh number, and also to a lower heat flux under the continental lid itself.

[51] We noted that the Biot number is the maximum heat flux that can be seen at the base of the continental lid. As was noted at the end of section 2, estimates of the Biot number for the Earth for whole mantle convection are between 8 and 20 for a continental lithosphere of thickness 330 km and 150 km, respectively. Using $k = 4$ W m^{-1} K^{-1} for the thermal conductivity of the continental lithosphere and of the mantle, and a superadiabatic temperature jump $\Delta T = 2500$ K across the mantle, these Biot numbers 8 and 20 correspond to maximum heat flux under the continent of 27 and 69 mW m^{-2}, respectively. Estimates of heat flux in oceanic regions are of the order of 100 mW m^{-2} [*Sclater et al.*, 1980]. The insulating effect of a 150 km thick lithosphere is thus moderate, while it is important for a 330 km thick lithosphere.

[52] The characteristics of convection under a lid of finite conductivity easily explain what is referred to as the Archean paradox, as was already pointed out by *Lenardic* [1998]. The Archean paradox refers to the fact that geochemical data in Archean rocks suggest that Archean continental geothermal gradients were not much different from the present ones [*Bickle*, 1978; *England and Bickle*, 1984; *Boyd et al.*, 1985], while the mantle was hotter and thus, according to common thinking, less viscous, yielding a more vigorous convection. Higher heat flux is then expected a priori. However, if one considers that the continental lithosphere had a thickness close to the present one, then the maximum heat flux that can be lost through continents is

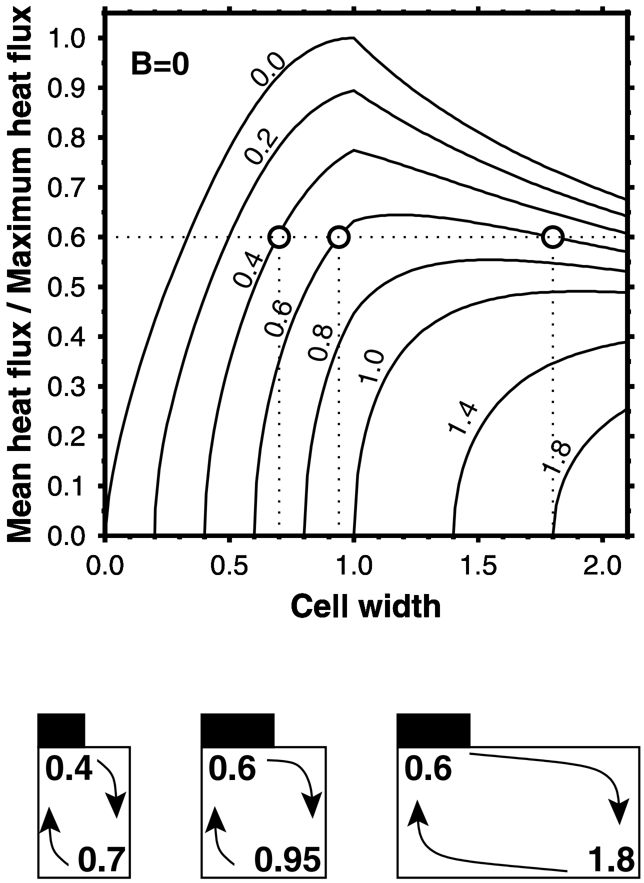

Figure 17. Mean heat flux normalized by the maximum heat flux obtained for cells of aspect ratio 1 with no continent, as a function of the width of the convective cell, for a perfectly insulating lid. The numbers along the curve indicate the width of the lid. The three circles correspond to the three configurations presented at the bottom, where the bold numbers indicate the widths of the lid and of the convective cell.

imposed by this lithospheric thickness, and can be estimated via the Biot number. High continental geothermal gradients, even with a vigorously convective mantle, cannot be obtained. This simple reasoning, as well as the scaling law proposed in section 5.2 and the results of the experiments carried out through this study, show that a large ratio between the oceanic heat flux and the continental heat flux can easily be obtained at high Rayleigh numbers. At $Ra = 10^8$, for a finitely conducting lid covering one third of the surface of a model of aspect ratio 4, the ratio between the oceanic heat flux and the continental heat flux is close to 6 for $B = 20$ and 13 for $B = 8$. Large oceanic heat flux can be obtained, while the continental heat flux remains close to the present one.

[53] Setting heterogeneous boundary conditions on top of a convective fluid, with a conductive zone through which the heat loss is limited, naturally generates a contrast in the heat loss between the free zone and the zone under the lid. For a given thermal conductivity and thickness of the conductive lid, this contrast increases with the Rayleigh number, and obtaining a low heat flux in the conductive zone and a high heat flux in the free zone is not a paradox.

6.2. Modification of the Pattern of Convection

[54] In all experiments carried out through this study, a hot zone of upwelling was obtained under the continental lid, generating a cellular circulation on both sides of the lid. We recall that our models are simple, with an isoviscous fluid and no mechanical coupling between the fluid and the lid. This configuration is not realistic for the Earth's mantle, although some features observed for the case of a slow moving continent can be obtained in our models: The form of the heat flux at the surface of the model, low below the continental lid and showing a sharp increase at the edge of the continent, is a feature than can be seen at the margins of the African shield [*Lucazeau et al.*, 2004]. We can infer from our results that continents must have a first-order effect on the dynamics of the mantle, and help generate a long-wavelength circulation.

[55] In a previous study [*Grigné et al.*, 2005] we noted the first-order importance of the wavelength of convection on the efficiency of the heat transfer. We here proposed a scaling law for the heat flux on top of a fluid partially covered by a finite conductivity lid. The width *L* of the convective cells is a first-order parameter in our parameterization. The scaling law for the heat flux as a function of the width of the cell *L* and of the width of the continent, for the case of a perfectly insulating lid, is presented in Figure 17. It indicates that the same heat flux can be obtained for different configurations. Three possible configurations that lead to a mean heat flux equal to 60% of the heat flux obtained for a cell of aspect ratio 1 with no continent are for instance presented in Figure 17. It must then be emphasized that studying the insulating effect of a lid of finite conductivity, in terms of total heat transfer, cannot be complete without taking into account the geometry of the flow. Our scaling law does not, however, predict this geometry of the flow, but only expresses the heat transfer efficiency as a function of the obtained wavelength of the convection.

7. Discussion and Conclusions

[56] In this paper, a complete scaling for the heat transfer efficiency of a two-dimensional isoviscous fluid covered completely or partially by a finitely conducting lid was built. This scaling expresses the heat flux out of the model as a function of the Rayleigh number of the fluid, the width of the convective cells and the width of the conductive lid and its insulating effect, through the Biot number. The presence of a finite conductivity lid on top of the fluid changes the wavelength of convection in the model, and we showed that this effect was as important in reducing the heat transfer efficiency as the local insulating effect of the lid.

[57] Two regimes of convection were identified, distinguishable by the fact that upwellings under the conductive lid occur in the forms of one narrow simple plume or of a wide set of several plumes. The scaling law proposed in this paper applies straightforwardly for the heat flux (equation (22)), but the two regimes imply changes for the scaling of the temperature (equations (26) and (25)).

[58] The insulating effect of the lid is quantified by the Biot number. This dimensionless number gives a good

approximation of the maximum heat flux that can be lost through the lid. In the case of the Earth, if one assumes that the thermal conductivities of the continental lithosphere and of the mantle are the same, the Biot number is simply the ratio between the convective mantle thickness and the continental lithosphere thickness. The maximum heat flux that can be lost at the base of a continental lithosphere of thickness between 200 and 300 km ranges from 30 to 50 mW m^{-2} with this approach, independently of the vigor of convection in the mantle. According to most parameterized models of mantle cooling [e.g., *Christensen*, 1985; *Breuer and Spohn*, 1993; *Grigné and Labrosse*, 2001], the oceanic heat flux was higher in the past. Thus the ratio between oceanic and continental heat flux could easily have been over 10 times larger in the Archean than at present-day.

[59] The approach used in this paper is simple, using an isoviscous fluid, no internal heating, and no mechanical coupling between the fluid and the lid, which allowed a quantitative systematic study and the construction of a parameterization. The introduction of internal heating within the continents can be expected to enhance the insulating effect of continents. The continental crust is indeed enriched in radioactive elements, and the internal heating rate in the continents is most probably at least 10 times larger than the one in the mantle. Introducing such internal heating rates in our models will lead to higher temperatures inside the lid and lower heat flux at its base. At $Ra = 10^7$, the heat flux under a partial lid of width 1 and with a Biot number $B = 10$ is 7.5 with no internal heating in the lid. It decreases to 3.7 when a dimensionless heating rate of 100 is introduced in the lid. In dimensional form, if we consider whole mantle convection with a continental lithosphere with the same thermal conductivity as the mantle and a thickness of 290 km, corresponding to a Biot number of 10, the value of 7.5 with no internal heating in the lid corresponds to 26 mW m^{-2}. The dimensionless internal heating rate of 100 corresponds to 0.1 μW m^{-3}, and the heat flux under the lid is then 13 mW m^{-2}, a value close to what is obtained under the Canadian Shield [*Pinet et al.*, 1991; *Jaupart et al.*, 1998; *Jaupart and Mareschal*, 1999].

[60] The insulating effect of continents can also be enhanced by the fact that the continental lithosphere is not in a thermal steady state: Diffusive heat transfer inside the continental lithosphere has a timescale comparable to the half-lives of radiogenic elements inside continents (e.g., U, Th, K), and the resulting transient behavior can increase the temperature at the base of the continental lithosphere by up to 150 K compared to a steady state model, further lowering the heat flux at the base of the lithosphere [*Michaut and Jaupart*, 2004]. A mechanical coupling between the continental lid and the convective fluid will also increase the insulating effect of the lid in models: Rigid boundary conditions will apply under the lid, forming a stagnant zone in the upper part of the fluid, rendering the effective thickness of the lid larger than the one actually imposed at the surface of the model.

[61] The simplifications used in this paper must be kept in mind. The effect of a temperature-dependent viscosity needs to be taken into account. *Lenardic et al.* [2005] questioned the actual global insulating effect of continents: The thermal blanketing effect of continents, increasing mantle temperature and thus lowering its viscosity, could lead to a more rapid overturn of oceanic lithosphere and to higher oceanic heat flux than in the case with no continents. The presence of rigid oceanic plates at the surface of the mantle should be taken into account: Tectonic plates generates long convective wavelength, which has a strong effect on the heat transfer efficiency. The effect of the wavelength of the flow was already studied by *Grigné et al.* [2005] but with no continents, and the effect of thermally insulating continents in the context of tectonic plates remains to be studied. It is also possible that the global insulating effect of continents is exaggerated in two-dimensional models [*Lowman and Gable*, 1999], and it will be necessary to investigate how scaling laws presented here can be extended to three-dimensional models.

[62] It appears, however, that under a wide range of conditions, the presence of a lid of finite conductivity on top of a convective fluid leads to a particular pattern of convection, with a zone of upwelling under the lid and a large cellular circulation centered beneath the lid. This particular pattern strongly modifies the heat transfer efficiency, compared to convection with homogeneous top boundary conditions. The complete scaling law we presented here, taking into account the geometry of the flow, can be used as a reference for future studies with more complex rheologies.

Appendix A: Lateral Heat Transfer in a Conductive Lid

[63] The thermal boundary condition under a finitely conducting lid, given by equations (4) and (5), is valid only if no horizontal heat transfer occurs inside the conductive lid. This hypothesis is accurate for thin lids only. As was shown by *Hewitt et al.* [1980] and *Guillou and Jaupart* [1995], lateral transfer of heat within the lid reduces its insulating effect, and the effective insulation is not known a priori, but is a function of the form of the temperature field within the lid.

[64] We carried out a large number of numerical experiments to study the effect of the horizontal heat diffusion inside the lid on its insulating effect. Various thicknesses d_c and thermal conductivities k_c, leading to the same Biot number, were imposed. These tests were carried out for Rayleigh numbers ranging from 10^5 to 10^8, for lid thicknesses ranging from $0.05d$ to d and for conductivities between $0.5k$ and $100k$. For a lid covering the entire surface of the fluid and a given Biot number, the difference obtained for the mean temperature of the fluid T_i between a model with a lid of thickness $d_c = 0.1d$ and a model with $d_c = d$ is never larger than 1.1%. For the mean heat flux at the surface of the fluid, this difference does not exceed 4%. For the full lid case, the boundary condition is thus always well described simply by the Biot number, and indicating the thickness and conductivity of the lid is not required.

[65] For a partial lid, horizontal diffusion of heat within the lid has a more important effect. A higher temperature at the interface between the lid and the fluid is clearly obtained for a thinner less conductive lid than for a thicker more conductive one with the same Biot number. On the range of parameters for the experiments carried out during this study, the difference for the mean heat flux out of the whole surface between the case $d_c = 0.05d$ and the case $d_c = d$ is

less than 4%. The corresponding range for the mean temperature T_i does not exceed 1% of its value. The way the Biot number is imposed is not a critical parameter for the mean thermal state of the fluid. The combination [k_c, d_c] is much more important for the heat flux under the lid and for the thermal state of the lid itself. For instance, at $Ra = 10^7$, a heat flux three times larger is obtained for the combination [$k_c = 10k$, $d_c = d$] than for the one [$k_c = 0.5k$, $d_c = 0.05d$], both cases leading to the same a priori Biot number, as defined by equation (5). In all the experiments carried out, the difference between the combinations [$k_c = k$, $d_c = 0.1d$] and [$k_c = 0.5k$, $d_c = 0.05d$] never exceeds 20%.

[66] As indicated in section 2, we carry out experiments with lids whose thickness does not exceed $0.1d$. The equation of conduction of heat through the finite conductivity lid is fully resolved, and the lateral transfer of heat, though almost negligible with $d_c \leq 0.1d$, is taken into account in our algorithm.

[67] **Acknowledgments.** We wish to thank Associate Editor Steve Cohen and Adrian Lenardic and Julian Lowman for very constructive reviews. All figures have been produced using the Generic Mapping Tool of *Wessel and Smith* [1998]. This work was supported by the program "Intérieur de la Terre" of INSU and NSF grant EAR-022950. This is ETH contribution 1461 and IPGP contribution 2145.

References

Bickle, M. (1978), Heat loss from the Earth: A constraint on the Archaean tectonics from the relation between geothermal gradients and the rate of plate production, *Earth Planet. Sci. Lett.*, *40*, 301–315.

Bobrov, A., W. Jacoby, and V. Trubitsyn (1999), Effects of Rayleigh number, length and thickness of continent on time of mantle flow reversal, *J. Geodyn.*, *27*, 133–145.

Boyd, F., J. Gurney, and S. Richardson (1985), Evidence for a 150–200 km thick Archaean lithosphere from diamond inclusion thermobarometry, *Nature*, *315*, 387–389.

Breuer, D., and T. Spohn (1993), Cooling of the Earth, Urey ratios, and the problem of potassium in the core, *Geophys. Res. Lett.*, *20*, 1655–1658.

Chapman, C., and M. Proctor (1980), Nonlinear Rayleigh-Bénard convection between poorly conducting boundaries, *J. Fluid Mech.*, *101*, 759–782.

Chapman, C., S. Childress, and M. Proctor (1980), Long wavelength convection between non-conducting boundaries, *Earth Planet. Sci. Lett.*, *51*, 362–369.

Christensen, U. R. (1985), Thermal evolution models for the Earth, *J. Geophys. Res.*, *90*, 2995–3007.

Collerson, K. D., and B. S. Kamber (1999), Evolution of the continents and the atmosphere inferred from Th-U-Nb systematics of the depleted mantle, *Science*, *283*, 1519–1522.

Conrad, C., and B. Hager (1999), The thermal evolution of the Earth with strong subduction zones, *Geophys. Res. Lett.*, *26*, 3041–3044.

England, P., and M. Bickle (1984), Continental thermal and tectonic regimes during the Archaean, *J. Geol.*, *92*, 353–367.

Grigné, C., and S. Labrosse (2001), Effects of continents on Earth cooling: thermal blanketing and depletion in radioactive elements, *Geophys. Res. Lett.*, *28*, 2707–2710.

Grigné, C., S. Labrosse, and P. J. Tackley (2005), Convective heat transfer as a function of wavelength: Implications for the cooling of the Earth, *J. Geophys. Res.*, *110*, B03409, doi:10.1029/2004JB003376.

Guillou, L., and C. Jaupart (1995), On the effect of continents on mantle convection, *J. Geophys. Res.*, *100*, 24,217–24,238.

Guillou, L., J. Mareschal, C. Jaupart, C. Gariepy, G. Bienfait, and R. Lapointe (1994), Heat flow, gravity and structure of the Abitibi belt, Superior Province, Canada: Implications for mantle heat flow, *Earth Planet. Sci. Lett*, *122*, 103–123.

Gurnis, M. (1988), Large-scale mantle convection and the aggregation and dispersal of supercontinents, *Nature*, *332*, 695–699.

Gurnis, M., and S. Zhong (1991), Generation of long wavelength heterogeneity in the mantle by the dynamic interaction between plates and convection, *Geophys. Res. Lett.*, *18*, 581–584.

Hewitt, J., D. McKenzie, and N. Weiss (1980), Large aspect ratio cells in two-dimensional thermal convection, *Earth Planet. Sci. Lett.*, *51*, 370–380.

Honda, S., M. Yoshida, S. Ootorii, and Y. Iwase (2000), The timescales of plume generation caused by continental aggregation, *Earth Planet. Sci. Lett.*, *176*, 31–43.

Hurle, D., E. Jakeman, and E. Pike (1967), On the solution of the Bénard problem with boundaries of finite conductivity, *Proc. R. Soc. London, Ser. A*, *296*, 469–475.

Ishiwatari, M., S.-I. Takehiro, and Y.-Y. Hayashi (1994), The effects of thermal conditions on the cell sizes of two-dimensional convection, *J. Fluid Mech.*, *281*, 33–50.

Jaupart, C., and J. Mareschal (1999), The thermal structure and thickness of continental roots, *Lithos*, *48*, 93–114.

Jaupart, C., J. Mareschal, L. Guillou-Frottier, and A. Davaille (1998), Heat flow and thickness of the lithosphere in the Canadian Shield, *J. Geophys. Res.*, *103*, 15,269–15,286.

Korenaga, J. (2003), Energetics of mantle convection and the fate of fossil heat, *Geophys. Res. Lett.*, *30*(8), 1437, doi:10.1029/2003GL016982.

Lenardic, A. (1998), On the partitioning of mantle heat loss below oceans and continents over time and its relationship to the Archean paradox, *Geophys. J. Int.*, *134*, 706–720.

Lenardic, A., and L. Moresi (2003), Thermal convection below a conducting lid of variable extent: Heat flow scalings and two-dimensional, infinite Prandtl number numerical simulations, *Phys. Fluids*, *15*, 455–466.

Lenardic, A., L. Moresi, A. M. Jellinek, and M. Manga (2005), Continental insulation, mantle cooling, and the surface area of oceans and continents, *Earth Planet. Sci. Lett.*, *234*, 317–333, doi:10.1016/j.epsl.2005.01.038.

Lowman, J. P., and C. W. Gable (1999), Thermal evolution of the mantle following continental aggregation in 3D convection models, *Geophys. Res. Lett.*, *26*, 2649–2652.

Lowman, J. P., and G. T. Jarvis (1993), Mantle convection flow reversals due to continental collisions, *Geophys. Res. Lett.*, *20*, 2087–2090.

Lucazeau, F., F. Brigaud, and J. L. Bouroullec (2004), High-resolution heat flow density in the lower Congo basin, *Geochem. Geophys. Geosyst.*, *5*, Q03001, doi:10.1029/2003GC000644.

Michaut, C., and C. Jaupart (2004), Nonequilibrium temperatures and cooling rates in thick continental lithosphere, *Geophys. Res. Lett.*, *31*, L24602, doi:10.1029/2004GL021092.

Pinet, C., C. Jaupart, J. Mareschal, C. Gariepy, G. Bienfait, and R. Lapointe (1991), Heat flow and structure of the lithosphere in the Eastern Canadian Shield, *J. Geophys. Res.*, *96*, 19,941–19,963.

Rudnick, R., W. McDonough, and R. O'Connell (1998), Thermal structure, thickness and composition of continental lithosphere, *Chem. Geol.*, *145*, 395–411.

Sclater, J., C. Jaupart, and D. Galson (1980), The heat flow through oceanic and continental crust and the heat loss of the Earth, *Rev. Geophys.*, *18*, 269–311.

Sparrow, E., R. Goldstein, and V. Jonsson (1964), Thermal instability in a horizontal layer: Effect of boundary conditions and non-linear temperature profile, *J. Fluid. Mech.*, *18*, 513–528.

Tackley, P. J. (1993), Effects of strongly temperature-dependent viscosity on time-dependent, 3-dimensional models of mantle convection, *Geophys. Res. Lett.*, *20*, 2187–2190.

Trubitsyn, V., and V. Rykov (1995), A 3-D numerical model of the Wilson cycle, *J. Geodyn.*, *20*, 63–75.

Turcotte, D., and E. Oxburgh (1967), Finite amplitude convection cells and continental drift, *J. Fluid Mech.*, *28*, 29–42.

Turcotte, D., and G. Schubert (1982), *Geodynamics: Application of Continuum Physics to Geological Problems*, John Wiley, New York.

Wessel, P., and W. H. F. Smith (1998), New, improved version of Generic MappingTools released, *Eos Trans. AGU*, *79*(47), 579.

Yoshida, M., Y. Iwase, and S. Honda (1999), Generation of plumes under a localized high viscosity lid in 3D spherical shell convection, *Geophys. Res. Lett.*, *26*, 947–950.

Zhong, S., and M. Gurnis (1994), Role of plates and temperature-dependent viscosity in phase change dynamics, *J. Geophys. Res.*, *99*, 15,903–15,917.

C. Grigné and P. J. Tackley, Institut für Geophysik, ETH Zürich, ETH Hönggerberg HPP, Zürich CH-8093, Switzerland. (cecile.grigne@erdw.ethz.ch; ptackley@ethz.ch)

S. Labrosse, Sciences de la Terre, Ecole Normale Supérieure de Lyon, 46 Allée d'Italie, F-69364 Lyon Cedex 07, France. (stephane.labrosse@ens-lyon.fr)